Egyptian Journal of Chemistry
http://ejchem.journals.ekb.eg/

An innovative and environmentally benign approach involves the use of algae amino-modified nanoparticles to effectively remove phenol from water, resulting in considerable environmental benefits

Alaa M. Younis*, Rand A. N. Alkhalifa, Sayed M. Saleh
Department of Chemistry, College of Science, Qassim University, Buraidah 51452, Saudi Arabia

Abstract

This study presents a green and effective strategy for removing phenolic pollutants from aqueous systems by utilizing amino-modified *Sargassum angustifolium* nanoparticles (Amino-SANPs), a novel biosorbent engineered from abundant marine biomass. The innovative aspect of this work lies in the surface functionalization of naturally derived algae with amino groups, which significantly enhances adsorption properties by increasing surface area, increasing active site availability, and increasing the potential for hydrogen bonding and electrostatic interactions. Comparative experiments demonstrate that Amino-SANPs outperform unmodified SANPs, achieving a maximum phenol removal efficiency of 79%, with an adsorption capacity of 90 mg/g, as determined by the Langmuir isotherm model. Batch adsorption studies were conducted to investigate the impact of critical operational parameters, including pH, contact time, initial phenol concentration, and adsorbent dosage. Kinetic modeling revealed that the adsorption process followed a pseudo-second-order mechanism, indicating chemisorption dominated by surface interactions between phenol molecules and amino-functionalized active sites. SEM imaging further confirmed morphological enhancement after modification, with increased porosity and surface roughness contributing to efficient pollutant capture. Additionally, isotherm analyses using Langmuir and Freundlich models provided insight into monolayer and heterogeneous adsorption behavior, respectively, with high correlation coefficients supporting the robustness of the findings. This research demonstrates the potential of integrating nanotechnology with natural biosorbents to create cost-effective, regenerative, and high-performance materials for water purification. The use of renewable algal biomass not only adds value to marine waste streams but also aligns with the principles of a circular economy. Overall, the application of Amino-SANPs represents a sustainable and scalable solution for mitigating phenolic contamination in water systems, offering substantial environmental benefits through reduced chemical usage, lower energy demands, and enhanced ecological protection.

Keywords: Phenol removal; Wastewater; Treatment; Sargassum angustifolium; Hazardous; Adsorption.

1. Introduction

Globally, natural ecosystems and human health are increasingly threatened by environ-mental pollution, particularly from organic pollutants [1,2]. Aromatic hydrocarbons, phenols, and aldehydes are prominent examples of volatile organic compounds (VOCs) that arise from various industrial processes [3,4]. These compounds serve multiple pur-poses, including acting as reactive agents, solvents, and refrigerants. However, their un-controlled release poses significant risks to both the environment and human health. This can lead to serious health issues for humans and other animals, as well as detrimental ef-fects on aquatic ecosystems [5,6]. Phenol and its derivatives are common environmental pollutants, primarily arising from industrial activities such as petrochemical manufac-turing, pharmaceuticals, and waste disposal. Due to its toxicity and persistence in water bodies, effective removal of phenolic compounds from aqueous solutions is a critical con-cern for environmental protection and public health. Traditional methods for phenol re-moval, including chemical oxidation, biological degradation, and membrane filtration, often face challenges such as high operational costs, incomplete removal, and the genera-tion of secondary pollutants [7]. Recently, adsorption has gained attention as an efficient and cost-effective method for removing phenol from wastewater. Among various adsor-bents, bio-based materials have shown promising results. Algae, in particular, possess unique properties such as high surface area, abundant functional groups, and biodegra-dability, making them suitable candidates for adsorption processes. However, the low adsorption capacity of raw algal biomass can limit its practical application [8,9].

To enhance the adsorption capacity, researchers have explored the modification of algal biomass with nanoparticles. Nanoparticles can increase the surface area and introduce additional functional groups that facilitate the adsorption of phenolic compounds. This approach not only improves the efficiency of phenol removal but also promotes the utili-zation of renewable

---

*Corresponding author e-mail: A.Younis@qu.edu.sa.; (**Alaa M. Younis**).
Receive Date: 11 May 2025, Revise Date: 20 June 2025, Accept Date: 01 July 2025
DOI: 10.21608/ejchem.2025.379290.11750

resources [10]. The adsorption of phenol onto algal biomass is influ-enced by various factors, including the surface characteristics of the algae, the nature of the phenol compound, and environmental conditions such as pH [11]. Studies have indi-cated that the adsorption process primarily occurs through hydrophobic interactions, hy-drogen bonding, and electrostatic attraction between phenolic molecules and functional groups present on the algal surface [11]. Modification of algal biomass with nanoparticles can significantly enhance these interactions. Zhang et al. [12] demonstrated that the in-corporation of iron oxide nanoparticles into algal biomass improved the removal efficien-cy of phenol by increasing the surface area and providing additional active sites for ad-sorption. Similarly, Mader et al. [13] reported that silver nanoparticles not only augmented the adsorption capacity but also exhibited antimicrobial properties, which could be bene-ficial in treating contaminated water. Various types of nanoparticles have been utilized to modify algal biomass for phenol removal [10]. Metal oxides, such as iron oxide (Fe2O3) and titanium dioxide (TiO2), are frequently employed due to their stability and effective-ness in capturing phenolic compounds [14]. For example, Fe2O3 nanoparticles have been shown to enhance the adsorption capacity of Chlorella vulgaris by providing a larger sur-face area and improved interaction with phenol molecules [15].

Silica nanoparticles are among the many inorganic adsorption materials employed, and they have extraordinary features, including outstanding adsorption efficiencies [12,13, 16]. According to Xu et al. [17]; Wang et al. [18], they have a great deal of surface area and a high porosity, and their pore size distribution is similar throughout. Additionally, they have exceptional water dispersion, great mechanical stability, and thermal stability across a wide range of temperatures [19, 20]. These are only some of their remarkable physical and chemical qualities. Notable as well is the adaptability of their design. For instance, there are a great number of adsorption systems that are based on silica materials that are accessible for use in industrial applications. These systems include modified fluid nano- or micro-beads and batch approaches [21, 22]. As a result of the presence of reactive si-lanol groups, this material is non-toxic, economical, and provides a wide range of alterna-tives for surface modification. The surface silanol groups make it possible to immobilize a wide variety of organic and inorganic substances. Synthesizing various three- or two-dimensional forms or controlled coated particles, such as mesoporous, amorphous, gels, and fumed silica particles, is another significant feature [15, 23]. This may be accom-plished by converting the particles into a controlled coating. The surface of the nanoparti-cles and the whole pore surface of silica nanobeads may be readily adjusted by adding various functional groups. This allows the nanobeads to be manipulated straightfor-wardly. This makes it possible for the beads to attach themselves to various species or molecules in the media that surrounds them, either by a covalent or a static attachment [24]. Their effectiveness is improved by surface modification, which considers their chem-ical, physical, thermal, and mechanical qualities. Nanoparticles that have been modified with silica are utilized in a variety of procedures, such as electrochemical sensing, optical detection, drug administration, catalysis, and separation processes [25-29].

Temperature also plays a crucial role in adsorption processes. Elevated temperatures can increase the kinetic energy of phenol molecules, potentially enhancing their diffusion to the adsorbent surface [30]. However, excessive temperatures may lead to desorption or degradation of the adsorbent material. Therefore, a balance must be achieved to optimize the adsorption process. The integration of algae with nanoparticles presents a promising approach for the removal of phenol from wastewater. Also, its abundance along regional coastlines, high biosorption potential due to its natural polyfunctional surface chemistry, and the added value of converting marine waste into a functional nanomaterial were clearly articulated to justify its suitability for phenol removal. This study proposes SANP and Amino-SANP as novel, accessible, and cost-effective adsorbents for the removal of phe-nolic compounds. Several factors contribute to the potential of SANP and Amino-SANP as effective candidates for phenol elimination. To assess the adsorption performance, we will employ the most suitable adsorption isotherm model. Additionally, we will investigate the process parameters influencing the adsorption kinetics, including pH, initial phenol concentration, adsorbent dosage, and contact time.

2. Experimental

2.1 Materials

Sigma-Aldrich was the supplier of all the essential chemicals. All aqueous working solutions were prepared using bidistilled water. Tetraethyl orthosilicate (TEOS) with a purity of 98%, APTS (3- aminopropyl) trimethoxysilane with a purity of 97% and ammonium hydroxide solution with a concentration of 28% (NH3) were all taken from the Sigma-Aldrich Company and employed in their respective forms. The stock standard solutions, which included 1 g/L of phenol, were blended with bi-distilled water and stored in a dark glass container at degrees Celsius. Stock solutions were made with bi-distilled water to ensure that the requisite phenol concentrations were achieved. Fresh working solutions were created right before they were used in each experiment. This was accomplished by diluting the stock standard solution of phenol with bi-distilled water until it reached the chosen initial concentration.

2.2. Preparation of dried natural nanoparticles

The preparation of nanoparticles made from dried SANP after being taken from the water of the Red Sea coast, SANP were washed with stream water and then sterile distilled water to eliminate any debris that may have been present. Thereafter, they were allowed to dry at room temperature. Using an agate mortar, the dried SANP were subjected to mechanical pretreatment, crushing, and screening using analytical sieves. Before its utilization, a planetary ball mill was used to transform the excellent powder produced into nanoparticles (SANP).

2.3. Peparation of Amino-SANP

Preparation of silica-coated nanoparticles derived from SANP. The preparation of silica-coated SANP nanoparticles was conducted using the method established by Stober et al (1968). A mixture comprising 150 mg of SANP nanoparticles was stirred vigorously in 100 mL ethanol, 250 µL bi-distilled water, and 250 µL of 25% ammonia solution at 40 °C for 30 minutes. Subsequently, 100 µL of TEOS was added, and the mixture was stirred slowly for 4 hours under the same conditions. To introduce the coated SANP nanoparticle surface, 100 µL of APTS was added to the solution mixture and stirred gently for 4 hours at a constant rate of 150 rpm and at the same temperature. The nanoparticles were subjected to centrifugation and multiple washes with ethanol and acetone, followed by drying in a furnace at 60 °C.

2.4. Phenol stock solution

One milligram of ACS-grade phenol, obtained from Sigma Chemical Co., was dissolved in one liter of distilled and deionized water to prepare a stock solution of 1000 parts per million (mg/L). This stock solution was subsequently refrigerated for preservation. For the adsorption studies, aliquots of the stock solution were diluted to the desired concentrations for analysis.

2.5. Investigations on Biosorption in Batch Mode

To examine the effects of various parameters—such as adsorbent dose, contact time, pH, and initial concentration—on the adsorption efficiency of phenol onto SANP and Amino-SANP, batch mode experiments were conducted. The phenol adsorption experiments utilized 50 mL stoppered conical flasks. For each trial, 50 milligrams of SANP and Amino-SANP were added to 50 milliliters of aqueous solutions containing varying concentrations of phenol, and the mixtures were mechanically agitated at room temperature. Different time intervals were employed for sampling during the adsorption tests. Other parameters, including pH and initial phenol concentration, were held constant while investigating the influence of adsorbent dosage. Specifically, to assess the effect of adsorbent dosage, known quantities of SANP and Amino-SANP (50, 100, 150, and 250 mg) were shaken with an aqueous solution containing 50 mg/L of phenol for 24 hours.

Furthermore, batch sorption tests were conducted with varying initial concentrations of phenol (10, 50, 100, and 200 mg/L), while maintaining constant adsorbent dosage and contact time to evaluate the impact of initial concentration. Following the adsorption period, samples were collected from the Erlenmeyer flasks at predetermined intervals and filtered through 0.45-µm membrane filter paper (GF/C Whatman). The residual phenol concentrations were subsequently analyzed using a colorimetric method with a VIS/UV Spectrophotometer-19 (SCO-Tech, Germany) [31]. To minimize measurement errors, all experiments were performed in duplicate for 24 hours at room temperature (25 ± 2 °C). Average values were utilized for further calculations. To determine the amount of phenol ions removed during adsorption, negative controls (without adsorbent) were run concurrently. The quantity of adsorbed phenol, q_e (mg/g), onto SANP and Amino-SANP was calculated by determining the initial and equilibrium concentrations using the appropriate equation.

$$q_e = ((C_o-C_e)V)/m_s$$

The variables C_o (milligrams per liter), C_e (milligrams per liter), V (liters), and m_s (grams) represent the initial concentration of the metal solution, equilibrium metal concentration, volume of the solution, and mass of the adsorbent, respectively. **All** batch adsorption experiments were conducted in triplicate (n = 3) and the average values were reported.

Furthermore, we have included a brief discussion in the Results and Discussion section, acknowledging that while batch experiments are ideal for preliminary evaluations and parameter optimization (e.g., the effect of pH, dosage, and initial concentration), they may not fully replicate the hydrodynamic conditions of real-world treatment systems. We have noted that dynamic systems, such as fixed-bed or column studies, are more representative of practical applications. Future work will focus on validating the efficacy of SANP and Amino-SANP under continuous flow to assess scalability and long-term stability.

2.6. Isotherms for Biosorption

The equilibrium concentrations of phenol in an aqueous solution at room temperature with respect to SANP and Amino-SANP were evaluated using the Freundlich and Langmuir isotherm models. The Langmuir equation is expressed as:

$$C_e/Q_e = 1/(Q_{max} K_L) + C_e/Q_{max}$$

The Freundlich equation is given by:

$$\text{Log } Q_e = \log K_f + 1/n \text{ Log } C_e$$

These equations were employed to describe the adsorption behavior. In these formulations, C_e represents the equilibrium concentration of phenol in the aqueous phase, Q_{max} is the monolayer saturation specific adsorption capacity, and K_L and K_f are the Langmuir and Freundlich constants, respectively. Additionally, n is an empirical parameter that indicates the adsorption strength.

2.7. Rate of Biosorption

To assess the kinetics of phenol biosorption, kinetic studies were conducted using intraparticle diffusion, pseudo-first-order, and pseudo-second-order models. The equations for these models are as follows:

For the pseudo-first-order model:

$$\ln (q_e - q_t) = \ln q_e - k_1 t$$

For the pseudo-second-order model:

$$t/q_t = 1/k^2 q_e^2 + t/q_e$$

The parameters of the adsorption kinetics were determined by applying equations (1), (2), and (3). Here, q_e denotes the amount of phenol adsorbed at equilibrium, while qt represents the amount adsorbed at a specific contact time t. The rate constants k_1 (h^{-1}), and k_2 (mg/g h^{-1}), correspond to the pseudo-first-order, and pseudo-second-order respectively.

3. Results and discussion

3.1 Surface morphology and structural characteristics of Amino-Coated SANP

Fig. 1 presents an SEM image of amino-coated SANP, offering valuable insights into their surface morphology and structural characteristics. The surface appears granular with overlapping fragments, suggesting a high surface area that is beneficial for adsorption applications. The particle size distribution is non-uniform, with some regions showing compact aggregates. This aggregation may result from the coating process, where amino groups promote interparticle interactions through hydrogen bonding or electrostatic forces. The irregular morphology also indicates the retention of the original structural features of the SANP biomass, which may enhance its adsorption efficiency by providing diverse active sites.

Fig. 1: SEM Images of Amino-SANP Biomass Structure

The amino-coated nanoparticles exhibit a distinct layered structure in certain regions, possibly due to the deposition of functional groups during the coating process. The pres-ence of amino groups is expected to enhance the material's affinity for pollutants through electrostatic interactions. The roughness and porosity observed in the SEM image further suggest the material's potential for high adsorption capacity, as these features facilitate the diffusion of target molecules into the active sites [32].

Specifically, we emphasize that while the deployment of amino-modified algal nanoparticles presents a promising, low-cost, and biodegradable approach to phenol removal, their environmental fate must be carefully assessed. The small size and surface reactivity of nanoparticles could pose risks related to bioaccumulation or unintended interactions with non-target aquatic organisms. However, Sargassum angustifolium-derived particles are biologically based. They are expected to exhibit lower persistence and toxicity compared to synthetic nanomaterials, particularly when recovery and reuse protocols (e.g., filtration, immobilization) are employed before discharge. On the positive side, the removal of phenol, a persistent, bioaccumulative, and toxic organic pollutant, from aquatic systems confers significant ecological benefits, including reduced oxidative stress in aquatic fauna and enhanced ecosystem resilience. Furthermore, using marine biomass valorizes algal overgrowth in coastal areas and reinforces circular bioeconomy principles. We also note that future studies should assess the long-term ecotoxicological profile and transport behavior of SANPs and Amino-SANPs under various environmental conditions.

3.2. Effect of pH

Fig. 2 illustrates the impact of pH levels from 3 to 10 on the phenol removal effectiveness from aqueous solutions by SANP and amino-SANP at 25 ± 1°C during a duration of 24 hours, utilizing a phenol ion concentration of 50 mg/L and a shaking speed of 150 rpm with a biosorption dosage of 50 mg. Incorporating of amino groups into the surface of the SANPs is crucial in the phenol elimination process. The presence of amino groups on the Amino-SANP surface amplifies electrostatic interaction with negatively charged pheno-late ions, considerably enhancing the adsorption process's efficiency. Moreover, phenol molecules possess a pKa value of 9.95, resulting in the formation of phenoxide ions that provide a degree of stabilization, hence diminishing the adsorption process owing to repulsive interactions between SANPs or Amino-SANP and phenoxide ions. Under acidic circumstances, the whole positive charge on SANPs or Amino-SANP amplifies electrostatic attraction with phenolate ions, hence improving adsorption effectiveness. These findings align with contemporary research [33-35]. Ultimately, at pH 10, SANPs and Amino-SANP relinquish their positive charges, hence diminishing the efficacy of the ad-sorption process. As a result, adsorption effectiveness diminishes due to heightened repulsive interactions between SANPs and Amino-SANP and phenols, reducing adsorption.

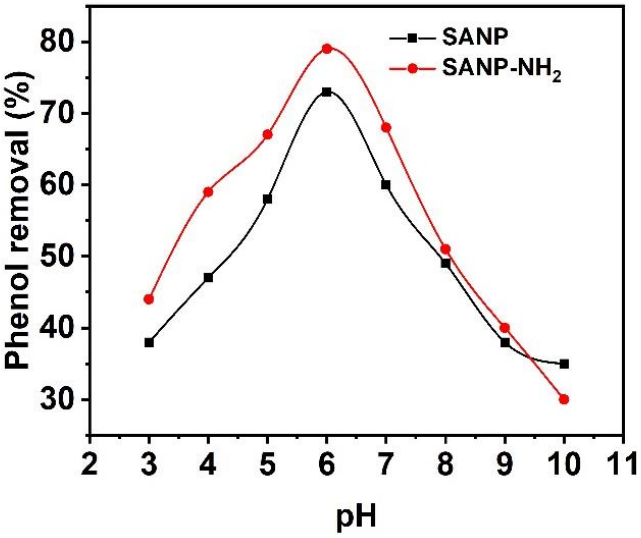

Fig. 2: Effect of initial pH on the phenol removal efficiency from aqueous solution vs pH of SANP and Amino-SANP.

3.3. Effect of contact time

Fig. 3 illustrates the effect of contact time on the adsorption of phenol from aqueous solutions using SANP and SANP-NH$_2$. The adsorption process shows a rapid initial increase in phenol removal, followed by a gradual approach to equilibrium. During the initial phase (0–8 hours), both adsorbents exhibit a sharp increase in phenol removal efficiency, indicating a fast adsorption rate. This rapid uptake can be attributed to the abundant availability of active adsorption sites on the nanoparticle surfaces, which readily interact with phenol molecules [36]. The adsorption rate slows down after 8 hours, as the available active sites become occupied, leading to a dynamic equilibrium between adsorption and desorption processes [37].

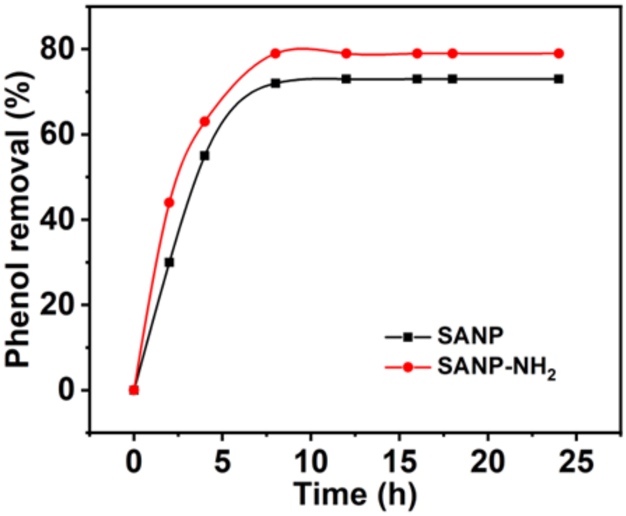

Fig. 3: Effect of Contact Time on Phenol Removal Using SANP and Amino-SANP

The results indicate that SANP-NH$_2$ outperforms SANP in phenol removal efficiency at all tested time points. At equilibrium, SANP achieves 73% phenol removal, whereas SANP-NH$_2$ reaches 79% removal. This enhancement in adsorption capacity can be at-tributed to the presence of amine functional groups (-NH$_2$), which provide additional active sites and improve phenol interaction through hydrogen bonding and electrostatic forces [38]. Functionalization with amine groups has been reported to enhance adsorption properties of various bio-based adsorbents [39]. Both adsorption systems reach equilibrium at approximately 12 hours, beyond which no significant increase in phenol removal is observed. This suggests that the active sites on the nanoparticles become saturated, and further contact time does not enhance adsorption capacity. The observed plateau aligns with pseudo-second-order kinetic models, which describe adsorption systems where chemisorption predominates [37]. The findings indicate that both SANP and SANP-NH$_2$ are effective adsorbents for phenol removal, with SANP-NH$_2$ demonstrating superior performance. The rapid adsorption kinetics, with most of the removal occurring within the first 8 hours, suggest that these materials could be suitable for wastewater treatment applications where efficient and fast removal of organic pollutants is required.

3.4. Effect of adsorbent dose

The effect of the adsorbent dose on the removal efficiency of phenol by SANP and SANP-NH$_2$ is illustrated in Fig. 4. The results indicate distinct trends in phenol removal efficiency with increasing adsorbent dose, reflecting the role of the surface chemistry and functionalization of the materials in the adsorption process. The removal efficiency of phenol by SANP increases steadily with the dose, reaching a plateau at 73% for doses of 100 mg and above. This trend suggests that the adsorption process stabilizes as the dose increases, likely due to the saturation of available active sites on the surface of SANP (Fig. 4). The plateau indicates that beyond 100 mg, additional adsorbent has minimal impact on further enhancing phenol removal, as most of the phenol molecules in the solution are already adsorbed. SANP-NH_2 demonstrates superior phenol removal efficiency compared to SANP at all doses tested. The removal efficiency increases sharply with the dose, reaching a maximum of 79% at a dose of 100 mg, and remains constant with further increases in dose. The enhanced performance of SANP-NH_2 can be attributed to the presence of amino (-NH_2) functional groups, which improve the adsorbent's affinity for phenol molecules through hydrogen bonding and electrostatic interactions [10,40,41].

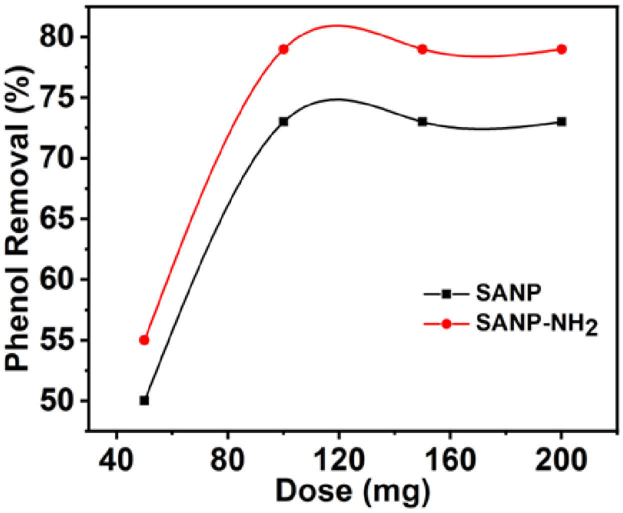

Fig. 4: Effect of adsorbent dose on Phenol Removal Using SANP and SANP-NH_2

The adsorption efficiency of both SANP and SANP-NH_2 reaches a plateau at a dose of 100 mg, indicating the saturation of active sites. At this point, the available phenol molecules in the solution are insufficient to occupy additional adsorption sites provided by higher doses. This observation highlights the importance of optimizing the adsorbent dose to balance removal efficiency and material usage.

3.5. Effect of phenol concentrations

Fig. 5 illustrates the effect of varying initial phenol concentrations (10-200 mg/L) on its removal efficiency using SANP and SANP-NH_2. The results reveal a decreasing trend in phenol removal efficiency with increasing initial phenol concentration for both adsorbents. At lower initial concentrations (10 mg/L), both SANP and SANP-NH_2 exhibit high adsorption efficiencies, achieving 73% and 79% removal, respectively. However, as the initial phenol concentration increases to 200 mg/L, the removal efficiency declines to 48% for SANP and 50% for SANP-NH_2. This inverse relationship is commonly observed in adsorption systems and can be attributed to the saturation of available active sites on the adsorbents [10,20].

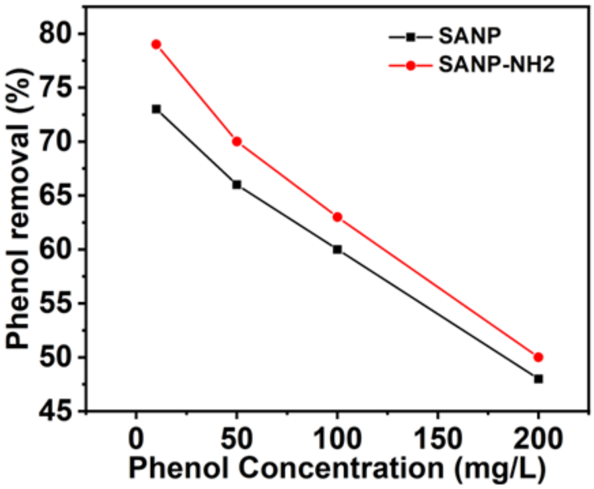

Fig. 5: Effect of phenol concentrations on Removal efficiency using SANP and SANP-NH_2

At lower concentrations, phenol molecules have a higher probability of interacting with and occupying available adsorption sites. However, as the concentration increases, the adsorbent surface becomes saturated, leading to a decrease in removal efficiency since a fixed number of adsorption sites are available [42]. Throughout the range of studied concentrations, SANP-NH_2 consistently outperforms SANP, demonstrating higher adsorption efficiency at all phenol concentrations. The enhanced adsorption capacity of SANP-NH_2 can be attributed to the presence of amine (-NH_2) functional groups, which provide additional active sites and improve phenol binding via hydrogen bonding and electrostatic interactions [20]. This supports previous findings that surface functionalization enhances the adsorption properties of bio-based materials [10]. The decreasing removal efficiency with increasing concentration also suggests that adsorption kinetics may transition from a rapid surface interaction (chemisorption) to a slower diffusion-controlled process at higher phenol concentrations [43].

The enhanced adsorption of phenol by SANP and especially Amino-SANP can be attributed to specific surface interaction mechanisms facilitated by the presence of functional groups. Phenol molecules, being weakly acidic and aromatic, interact with adsorbent surfaces through a combination of hydrogen bonding, π–π interactions, and electrostatic attractions. In the case of SANP-NH_2, the introduction of amino groups significantly enriches the adsorbent surface with electron-donating nitrogen sites capable of forming strong hydrogen bonds with the hydroxyl group of phenol. These amino functionalities also introduce positive surface charges at lower pH, promoting electrostatic attraction with deprotonated phenolate ions (especially near phenol's pKa of ~9.95). Moreover, the presence of surface roughness and increased porosity, as observed in the SEM analysis (Section 3.1), contributes to enhanced diffusion and entrapment of phenol molecules within the nanoparticle matrix.

Additionally, the heterogeneous active sites introduced through surface modification allow for multilayer adsorption behavior, complementing the monolayer interactions described by the Langmuir isotherm. These combined effects result in the superior adsorption performance of Amino-SANP over unmodified SANP, as further supported by kinetic data that conform to the pseudo-second-order model, indicating chemisorption dominated by electron-sharing mechanisms. Therefore, surface functionalization plays a pivotal role in tuning both the chemical affinity and physical accessibility of phenol adsorption sites.

3.6. Adsorption isotherms

The adsorption isotherm delineates the relationship between the equilibrium concentration of the adsorbate in the solid phase, which is statically bonded to the adsorbent sur-face, and in the liquid phase as a soluble component. This work was conducted at a constant temperature throughout the adsorption procedure [29]. The adsorption behavior of phenol onto SANP and SANP-NH_2 was systematically evaluated using equilibrium isotherms. These analyses provide a deeper understanding of the adsorption mechanism, capacity, and efficiency of the adsorbents.

Equilibrium isotherm models serve as fundamental tools for describing the interaction between phenol and the adsorbent surface at equilibrium. The Langmuir isotherm assumes a monolayer adsorption process on a homogeneous surface with a finite number of adsorption sites. In contrast, the Freundlich isotherm accounts for multilayer adsorption on heterogeneous surfaces, reflecting variations in adsorption energy across different sites. The Langmuir model parameters reveal key differences in adsorption performance between SANP and SANP-NH_2. The maximum adsorption capacity (q_m) for SANP-NH_2 (90 mg/g) is markedly higher than that of SANP (58 mg/g), emphasizing the significant enhancement imparted by amino (-NH_2) functionalization. The presence of these functional groups introduces additional active sites, thereby increasing the overall adsorption capacity without altering the intrinsic affinity for phenol molecules. This is further supported by the fact that both adsorbents exhibited identical Langmuir constant (K_l) values (0.004 mg/g), indicating comparable adsorption affinity under the given experimental conditions (Table 1).

Table 1. The isotherms of adsorption of phenol onto SANP and SANP-NH_2: Computed parameters and analysis

Equilibrium Model	Parameters	*SANP*	*SANP-NH_2*
Langmuir	q_m (mg. g^{-1})	58	90
	K_L (mg. g^{-1})	0.004	0.004
	R_L (L.mg^{-1})	0.95	0.96
	R^2	0.9997	0.9999
Freundlich	n	1.05	1
	K_F (L.mg^{-1})	1.01	1.009
	R^2	0.999	0.999

The separation factor (R_l), a crucial indicator of adsorption favorability, remained close to 1 for both SANP (0.95) and SANP-NH_2 (0.96), suggesting that the adsorption process is favorable across the tested concentration range. Furthermore, the Langmuir model demonstrated an exceptional fit for both SANP ($R^2 = 0.9997$) and SANP-NH_2 ($R^2 = 0.9999$), reinforcing the notion that phenol adsorption predominantly follows a monolayer adsorption mechanism on a homogeneous surface. Conversely, the Freundlich model accounts for surface heterogeneity and variable adsorption energies [44, 45].

The heterogeneity factor (n) for SANP (1.05) and SANP-NH_2 (1.0) indicates nearly linear adsorption behavior, with minimal deviation from ideal conditions. This suggests that while SANP-NH_2 exhibits a higher adsorption capacity, the functionalization does not significantly alter surface heterogeneity. Additionally, the Freundlich constant (K_x) values for SANP (1.01 L/mg) and SANP-NH_2 (1.009 L/mg) were nearly identical, implying similar adsorption intensity. Both adsorbents showed an excellent fit to the Freundlich model ($R^2 = 0.999$), suggesting the possibility of a heterogeneous adsorption process coexisting with monolayer adsorption (Fig. 6)

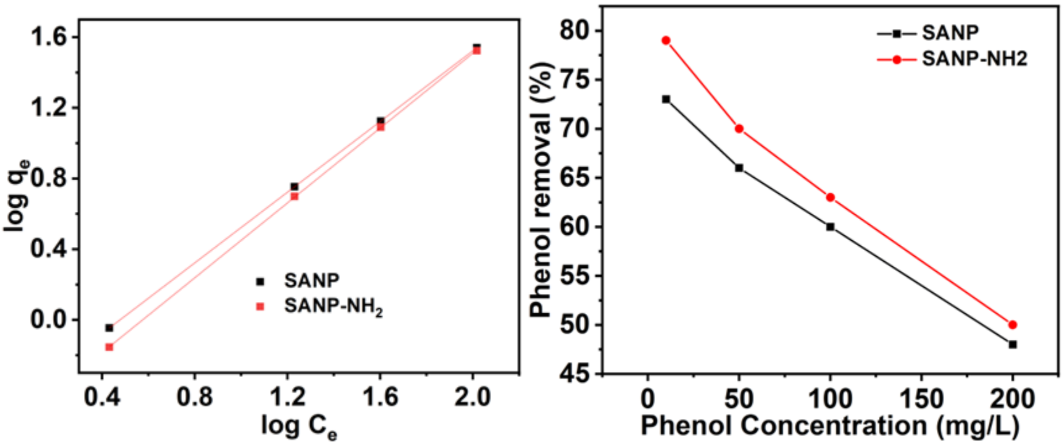

Fig. 6: The linear fitting results for the Langmuir and Freundlich isotherm models

The comparative analysis underscores the key role of amino functionalization in enhancing adsorption capacity while maintaining adsorption affinity and surface characteristics. The superior q_m of SANP-NH_2 validates the hypothesis that surface functionalization introduces additional active sites, thereby increasing the adsorption potential. However, the nearly identical K_l, K_x, and n values suggest that the overall adsorption mechanism remains unchanged, with both adsorbents following a predominantly monolayer adsorption process with minor contributions from multilayer adsorption. These findings align with previous studies demonstrating that surface modification with functional groups enhances adsorption performance without drastically altering the fundamental adsorption mechanism [10,20,46]. The results provide a scientific foundation for the development of functionalized biosorbents as efficient and sustainable materials for water purification applications.

3.7. Adsorption kinetics

The dynamic behavior of phenol adsorption onto SANP and SANP-NH_2 was scrutinized using the pseudo-first-order (PFO) and pseudo-second-order (PSO) models. These models serve as critical tools to uncover the intricate adsorption mechanisms, encompassing diffusion and chemical interactions, thereby furnishing a holistic comprehension of the ad-sorption process. The PFO model operates under the assumption that the adsorption rate is proportional to the disparity between the equilibrium adsorption capacity (q_e) and the adsorbate amount adsorbed at time t. Nevertheless, its application to the phenol adsorption onto SANP and SANP-NH_2 unveiled several constraints. The experimentally derived qe values for SANP (4.13 mg/g) and SANP-NH_2 (7.07 mg/g) markedly deviated from the Langmuir isotherm predictions, indicating subpar concordance between the PFO model and the empirical data (Table 2). This discrepancy implies the PFO model's inadequacy in accurately delineating the phenol adsorption kinetics onto these substrates. The exceed-ingly low k_1 values for SANP (0.00004 L/min) and SANP-NH_2 (0.00002 L/min) pointed to a sluggish adsorption process when scrutinized through the PFO model, underscoring its inefficacy in elucidating the adsorption mechanism effectively.

Table 2. Kinetic modeling of phenol adsorption onto SANP and SANP-NH_2: Computational parameters and analysis

rameters and analysis

Kinetics Models	Variables	Parameters Unit	*SANP*	*SANP-NH₂*
PFO	q_e	*mg/g*	4.13	7.07
	k_1	*L/min*	0.00004	0.00002
	R^2	-	0.54	0.54
PSO	$q_{e\,(calculated)}$	*mg/g*	32	43
	k_2	*mg/mg.min*	0.003	0.004
	R^2	-	0.996	0.997

Both SANP and SANP-NH_2 exhibited R^2 values of 0.54, signaling a deficient fit of the PFO model to the experimental data (Fig. 7a). This discrepancy implies that the phenol adsorp-tion is not primarily steered by a simplistic diffusion-mediated process as postulated by the PFO model. In contrast, the PSO model predicates that the adsorption rate is contin-gent upon the chemical interactions between the adsorbate (phenol) and the adsorbent surface. Evaluation using the PSO model proffered a markedly superior portrayal of the adsorption kinetics for both SANP and SANP-NH_2.

The PSO model foretold qe values of 32 mg/g for SANP and 43 mg/g for SANP-NH_2, aligning closely with the experimental findings and Langmuir isotherm outcomes, signi-fying the PSO model's apt depiction of the adsorption mechanism, predominantly gov-erned by chemisorption. The k_2 values for SANP (0.003 mg/mg.min) and SANP-NH_2 (0.004 mg/mg.min) suggested marginally accelerated adsorption kinetics for SANP-NH_2. The incorporation of amino functional groups bolstered the chemical interactions between phenol and the adsorbent surface, augmenting the adsorption efficacy of SANP-NH_2. No-tably, the R^2 values derived from the PSO model were notably high (0.996 for SANP and 0.997 for SANP-NH_2), affirming the model's superior fitting and indicating that the ad-sorption process is predominantly steered by chemisorption mechanisms involving elec-tron sharing or exchange (Fig. 7b).

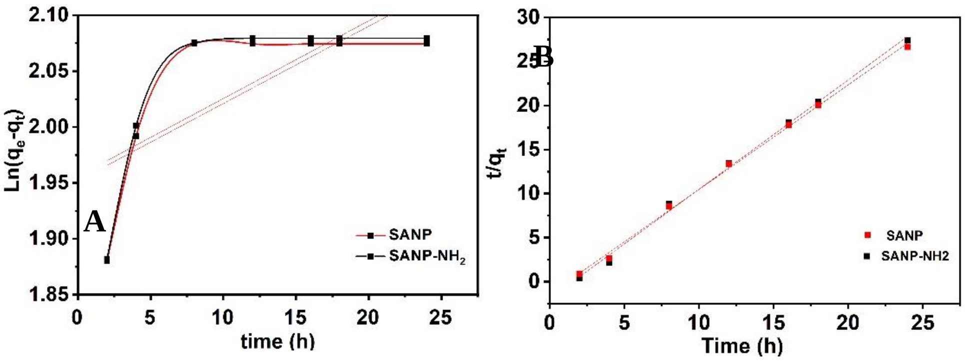

Fig. 7: Linearized Kinetic Models for Phenol Adsorption: (a) PFO and (b) PSO

4. Conclusion

This study demonstrated the effective use of dried and amino-modified Sargassum angustifolium nanoparticles (SANPs and Amino-SANPs) for the adsorption of phenol from aqueous media. Amino-functionalization significantly enhanced the adsorption efficiency, as evidenced by superior performance in kinetic and isotherm models, with the Langmuir model indicating a maximum adsorption capacity of 90 mg/g for Amino-SANPs. The adsorption process followed pseudo-second-order kinetics, confirming the chemisorption nature of the interaction between phenol molecules and functionalized algal surfaces. In addition to their environmental compatibility and cost-effectiveness, these biosorbents show strong potential for development into sustainable water purification technologies. Although regeneration studies were not performed in the current work, the observed structural stability and reusability potential of algal-based nanomaterials merit further exploration. Future research should investigate regeneration cycles, column-based continuous adsorption systems, and the optimization of synthesis protocols for large-scale production. Furthermore, the application of SANPs and Amino-SANPs could be extended to the removal of other emerging contaminants such as pharmaceuticals, dyes, and endocrine-disrupting compounds.

5. Conflicts of interest

The authors declare no conflicts of interest.

6. Formatting of funding sources

"The authors gratefully acknowledge Qassim University, represented by the Deanship of Graduate Studies and Scientific Research, on the financial support for this research under the number (QU-J-PG-2-2025-5165) during the academic year 1446 AH / 2024 AD".

7. Acknowledgment

"The authors gratefully acknowledge Qassim University, represented by the Deanship of Graduate Studies and Scientific Research, on the financial support for this research under the number (QU-J-PG-2-2025-56165) during the academic year 1446 AH / 2024 AD".

8. References

[1] Elkady, E.M. and A.M. Younis, The potential accumulation of polycyclic aromatic hydrocarbons in macroalgae from the Egyptian coast of the Red Sea. Egyptian Journal of Aquatic Research, 2023. 49(4): p. 452-459.

[2] Younis, A.M., et al., Assessment of health risks associated with heavy metal contamination in selected fish and crustacean species from Temsah Lake, Suez Canal. Scientific Reports, 2024. 14(1): p. 18706.

[3] Younis, A.M., E.M. Elkady, and M. El-Naggar, Biosorption of Arsenic (III) and Arsenic (V) from Aqueous Solutions: Equilibrium and Kinetic Studies using Mangrove Leaf Biomass (Avicennia marina). Egyptian Journal of Aquatic Biology & Fisheries, 2023. 27(6).

[4] El-Naggar, M., et al., Seasonal and temporal influence on polycyclic aromatic hydrocarbons in the Red Sea coastal water, Egypt. Sustainability, 2021. 13(21): p. 11906.

[5] Benouis, K., Khane, Y., Ahmed, T., Albukhaty, S. and Banoon, S.R., 2022. Valorization of diatomaceous earth as a sustainable eco-coagulant for wastewater treatment: optimization by response surface methodology. *Egyptian Journal of Chemistry*, *65*(9), pp.777-788.

6] Younis, A.M., A.M. Mostafa, and E.M. Elkady, Assessment of bioaccumulation and health risks of heavy metals in selected fish species from Red Sea coastal waters, Saudi Arabia. Egyptian Journal of Aquatic Research, 2024. 50(3): p. 348-356.

[7] Alkhalifa, R.A., et al., Sustainable Synthesis of Zirconium Dioxide (ZrO2) Nanoparticles Utilizing Asphodelus fistulosus Extract for Congo Red Degradation. Catalysts, 2025. 15(2): p. 123.

[8] Ren, B., et al., A comprehensive review on algae removal and control by coagulation-based processes: mechanism, material, and application. Separation and Purification Technology, 2022. 293: p. 121106.

[9] Younis, A.M., et al., Enteromorpha compressa Macroalgal Biomass Nanoparticles as Eco-Friendly Biosorbents for the Efficient Removal of Harmful Metals from Aqueous Solutions. Analytica, 2024. 5(3): p. 322-342.

[10] Younis, A.M., E.M. Elkady, and S.M. Saleh, Novel eco-friendly amino-modified nanoparticles for phenol removal from aqueous solution. Environmental Science and Pollution Research, 2020. 27(24): p. 30694-30705.

[11] Elkady, E.M., A.M. Younis, and M.H. El-Naggar, Investigating the Biosorption Potential of Ulva intestinalis Linnaeus for Efficient Removal of Phenol from Aqueous Solutions. Egyptian Journal of Aquatic Biology & Fisheries, 2023. 27(6).

[12] Zhang, W., et al., Fluorescent proteins as efficient tools for evaluating the surface PEGylation of silica nanoparticles. Methods and applications in fluorescence, 2017. 5(2): p. 024003.

[13] Mader, H., et al., Fluorescent silica nanoparticles. Annals of the New York Academy of Sciences, 2008. 1130(1): p. 218-223.

[14] Dehmani, Y., et al., Review of phenol adsorption on transition metal oxides and other adsorbents. Journal of water process engineering, 2022. 49: p. 102965.

[15] Singh, L.P., et al., Sol-Gel processing of silica nanoparticles and their applications. Advances in colloid and interface science, 2014. 214: p. 17-37.

[16] Saleh, S.M., R. Ali, and O.S. Wolfbeis, New silica and polystyrene nanoparticles labeled with longwave absorbing and fluorescent chameleon dyes. Microchimica Acta, 2011. 174: p. 429-434.

[17] Hassan, S.A.D.H., Almaliki, M.N.S., Hussein, Z.A., Albehadili, H.M., Rabeea Banoon, S., Abboodi, A. and Al-Saady, M., 2023. Development of nanotechnology by artificial intelligence: a comprehensive review. *Journal of Nanostructures*, *13*(4), pp.915-932.

[18] Wang, S., et al., Adsorption of Pb2+ on amino-functionalized core–shell magnetic mesoporous SBA-15 silica composite. Chemical Engineering Journal, 2015. 262: p. 897-903.

[19] Thommes, M., et al., Physisorption of gases, with special reference to the evaluation of surface area and pore size distribution (IUPAC Technical Report). Pure and applied chemistry, 2015. 87(9-10): p. 1051-1069.

[20] Saleh, S., et al., Phenol removal from aqueous solution using amino modified silica nanoparticles. Korean Journal of Chemical Engineering, 2019. 36: p. 529-539.

[21] Karim, A.H., et al., Amino modified mesostructured silica nanoparticles for efficient adsorption of methylene blue. Journal of colloid and interface science, 2012. 386(1): p. 307-314.

[22] Zargartalebi, M., R. Kharrat, and N. Barati, Enhancement of surfactant flooding performance by the use of silica nanoparticles. Fuel, 2015. 143: p. 21-27.

[23] Sun, B., et al., Reduction of acute inflammatory effects of fumed silica nanoparticles in the lung by adjusting silanol display through calcination and metal doping. ACS nano, 2015. 9(9): p. 9357-9372.

[24] Perez, G., et al., Synthesis and characterization of epoxy encapsulating silica microcapsules and amine functionalized silica nanoparticles for development of an innovative self-healing concrete. Materials Chemistry and Physics, 2015. 165: p. 39-48.

[25] Saleh, S.M., et al., Novel multicolor fluorescently labeled silica nanoparticles for interface fluorescence resonance energy transfer to and from labeled avidin. Analytical and bioanalytical chemistry, 2010. 398(4): p. 1615-1623.

[26] Gawande, M.B., et al., Silica-decorated magnetic nanocomposites for catalytic applications. Coordination Chemistry Reviews, 2015. 288: p. 118-143.

[27] Hosseini, S., et al., Electrodialysis heterogeneous ion exchange membranes modified by SiO2 nanoparticles: fabrication and electrochemical characterization. Water Science and Technology, 2016. 73(9): p. 2074-2084.

[28] Alminderej, F.M., et al., The superior adsorption capacity of phenol from aqueous solution using Modified Date Palm Nanomaterials: A performance and kinetic study. Arabian Journal of Chemistry, 2022. 15(10): p. 104120.

[29] Alsehli, B.R., et al., Biosynthesis, characterizations, and comparison of TiO2/CeO2/their nanocomposites as bio-adsorbents of linezolid and their microbiological activities. Journal of Molecular Structure, 2025. 1328: p. 141388.

[30] Yousef, R.I., B. El-Eswed, and H. Ala'a, Adsorption characteristics of natural zeolites as solid adsorbents for phenol removal from aqueous solutions: kinetics, mechanism, and thermodynamics studies. Chemical engineering journal, 2011. 171(3): p. 1143-1149.

[31] Martin, R., Rapid colorimetric estimation of phenol. Analytical chemistry, 1949. 21(11): p. 1419-1420.

[32] Zhang, W., et al., Microbial targeted degradation pretreatment: a novel approach to preparation of activated carbon with specific hierarchical porous structures, high surface areas, and satisfactory toluene adsorption performance. Environmental science & technology, 2019. 53(13): p. 7632-7640.

[33] Mirian, Z.-A. and A. Nezamzadeh-Ejhieh, Removal of phenol content of an industrial wastewater via a heterogeneous photodegradation process using supported FeO onto nanoparticles of Iranian clinoptilolite. Desalination and Water Treatment, 2016. 57(35): p. 16483-16494.

[34] Yang, G., et al., Simultaneous removal of lead and phenol contamination from water by nitrogen-functionalized magnetic ordered mesoporous carbon. Chemical Engineering Journal, 2015. 259: p. 854-864.

[35] Asmaly, H.A., et al., Ferric oxide nanoparticles decorated carbon nanotubes and carbon nanofibers: from synthesis to enhanced removal of phenol. Journal of Saudi Chemical Society, 2015. 19(5): p. 511-520.

[36] M Younis, A., M. A Aly-Eldeen, and E. M Elkady, Effect of different molecular weights of chitosan on the removal efficiencies of heavy metals from contaminated water. Egyptian Journal of Aquatic Biology and Fisheries, 2019. 23(4): p. 149-158.

[37] Rashid, M.K., Salman, I.R., Obaid, A.L., Hassan, S.A.D.H., Al-musawi, M.R. and Al-Saady, M., 2024. Application of machine learning in predicting sources of water pollution in the Euphrates and Tigris rivers in Iraq. *International Journal of Aquatic Biology*, *12*(6), pp.581-589.

[38] Ma, X., et al., DFT study of CO2 adsorption across a CaO/Ca12Al14O33 sorbent in the presence of H2O under calcium looping conditions. Chemical Engineering Journal, 2019. 370: p. 10-18.

[39] Memon, A.G., et al., Ultrasensitive colorimetric aptasensor for Hg2+ detection using Exo-III assisted target recycling amplification and unmodified AuNPs as indicators. Journal of Hazardous Materials, 2020. 384: p. 120948.

[40] Liu, B., et al., Adsorption of phenol and p-nitrophenol from aqueous solutions on metal–organic frameworks: effect of hydrogen bonding. Journal of Chemical & Engineering Data, 2014. 59(5): p. 1476-1482.

[41] Rasuli, L., et al., A novel amino acid functionalized biosorbent (almond shells) for the removal of phenol from aqueous solutions: linear and nonlinear kinetic models and thermodynamic studies. Biomass Conversion and Biorefinery, 2024: p. 1-13.

[42] Loganathan, P., S. Vigneswaran, and J. Kandasamy, Enhanced removal of nitrate from water using surface modification of adsorbents–a review. Journal of environmental management, 2013. 131: p. 363-374.

[43] De la Luz-Asunción, M., et al., Adsorption of phenol from aqueous solutions by carbon nanomaterials of one and two dimensions: Kinetic and equilibrium studies. Journal of Nanomaterials, 2015. 2015(1): p. 405036.

[44] Joseph, L., et al., Adsorption of bisphenol A and 17α-ethinyl estradiol on single walled carbon nanotubes from seawater and brackish water. Desalination, 2011. 281: p. 68-74.

[45] Alharbi, F.K., et al., Impact of Ag-NiO nanoparticles loaded on g-C3N4 nanosheets for cleaning contaminated water. Inorganic Chemistry Communications, 2024. 166: p. 112608.

[46] Jain, M., et al., Modelling and statistical interpretation of phenol adsorption behaviour of 3-Dimensional hybrid aerogel of waste-derived carbon nanotubes and graphene oxide. Chemical Engineering Journal, 2024. 490: p. 151351.